Int J Clin Exp Med 2026;19(6):152-167
www.ijcem.com /ISSN:1940-5901/IJCEM0167798

*Original Article*

# A novel survival model utilizing N6-Methyladenosine (m6A) modification regulators for prognostic prediction in renal cell carcinoma

Jing Yang[1,2,3], Yue Yang[4], Yuanhong Xiong[4], Haifeng Hu[4], Jin Yang[4], Yunhan Wang[4]

*[1]Department of Gastroenterology Nursing, West China Second University Hospital, Sichuan University, Chengdu 610041, Sichuan, China; [2]Key Laboratory of Birth Defects and Related Diseases of Women and Children (Sichuan University), Ministry of Education, Chengdu 610041, Sichuan, China; [3]WCSUH-Tianfu-Sichuan Provincial Children's Hospital, Meishan 610095, Sichuan, China; [4]Affiliated Hospital of Chengdu University, Chengdu 610081, Sichuan, China*

Received July 30, 2025; Accepted April 3, 2026; Epub June 15, 2026; Published June 30, 2026

**Abstract:** Objective: This study aimed to investigate the prognostic significance of m6A RNA methylation regulators in renal cell carcinoma (RCC) and to construct a predictive model. Methods: Based on The Cancer Genome Atlas (TCGA) database, we analyzed the expression of 19 m6A regulators in 883 RCC patients. Through survival analysis, consensus clustering, immune infiltration estimation, multivariate Cox regression, and enrichment analysis, we screened key regulators and assessed their clinical value. Results: The expression levels of four m6A regulators - METTL14, WTAP, RBM15B, and IGF2BP3 - were significantly associated with the overall survival of RCC patients. A prognostic model developed using these four regulators effectively categorized patients into high-risk and low-risk groups (hazard ratio [HR]=3.013, *p*-value =1.12e-13). Further analysis indicated that these regulators are implicated in key signaling pathways, including mTOR, VEGF, Wnt, and p53. Estimations of immune infiltration suggested their potential role in modulating the tumor microenvironment. Conclusion: METTL14, WTAP, RBM15B, and IGF2BP3 are potential prognostic biomarkers for RCC. The established predictive model demonstrates significant clinical utility, and the mechanisms may involve the regulation of the tumor microenvironment and key oncogenic pathways.

**Keywords:** N6-Methyladenosine (m6A), renal cell carcinoma, prognosis, biomarker, bioinformatics analysis

## Introduction

Renal cell carcinoma (RCC) is a malignant and insidious form of kidney cancer, ranking as the seventh most common neoplasm in the developed world [1]. According to the latest cancer database, approximately 400,000 people are diagnosed with RCC annually, and this number is rapidly increasing. In 2020, there were 73,750 new cases and 14,830 deaths from kidney cancer in America, with RCC accounting for 2.4% of all cancer-related deaths [2]. RCC has increasingly threatened human health due to its poor prognosis. It is reported that up to 17% of patients have at least one distant metastasis at the time of diagnosis, leading to high mortality. Surgery is recommended as the most effective treatment, but 20%-40% of RCC patients experience postoperative progression, such as metastasis or recurrence [3]. Therefore, identifying significant biomarkers and systematically assessing the prognosis of RCC could aid in the early application of various adjuvant therapies, contributing to an increased survival rate.

### *Background of m6A regulators*

N6-Methyladenosine (m6A) modification is one of the most common internal modifications on eukaryotic messenger RNA [4]. It involves methylation at the N6 position of adenosine and is implicated in various RNA functions, including the processing of primary microRNA, mRNA stability, splicing, transport, and translation. The m6A modification is identified by m6A binding proteins, catalyzed by m6A methyltransferases, and removed by m6A demethylases, par-

https://doi.org/10.62347/NNMI6196

ticipating in all metabolic processes of mRNA [5-8]. These processes are collectively referred to as the "reader", "writer", and "eraser" mechanisms.

The "readers" can be categorized into three types [9]: the first includes proteins with an evolutionarily conserved YTH domain (YT521-B homology), such as YTHDC1, YTHDC2, YTHDF1, YTHDF2, and YTHDF3; the second type contains three heterogeneous nuclear ribonucleoproteins (hnRNPs): hnRNPC, hnRNPG, and hnRNPA2B1; and the third type consists of insulin-like growth factor 2 mRNA-binding proteins 1-3 (IGF2BP1-3). The "writers", also known as methyltransferases, include METTL3 (methyltransferase-like 3), METTL14, METTL16, WTAP (Wilms' tumor 1-associating protein), VIRMA (Vir-like m6A methyltransferase associated), RBM15 (RNA-binding motif protein 15), Zc3h13 (Zinc finger CCCH-type containing protein 13), and Hakai [10]. The "erasers" are two demethylases, FTO and ALKBH5, which remove m6A modifications from mRNA [11, 12].

All m6A regulators, including "writers", "erasers", and "readers", play significant roles in cancers. Growing evidence suggests that m6A methylation disorders are directly associated with abnormal RNA metabolism, leading to tumor occurrence and changes in drug response. In Yongsheng Li's study [13], they systematically analyzed 20 m6A modulators across over 10,000 subjects representing 33 types of cancer and demonstrated an intimate connection between m6A regulators and the activation and inhibition of cancer pathways.

*Related studies of m6A in RCC*

Recently, Xiao Li et al. demonstrated that METTL3 might play a carcinomatous role in the proliferation, migration, invasion, and cell cycle of RCC cells and could act as a novel marker for RCC [14]. More evidence suggests that m6A could participate in the tumorigenesis of RCC [15, 16], but few studies have reached a consensus on specific m6A modulators that might play key roles in RCC [17-19]. In this study, we collected 883 patients with RCC from The Cancer Genome Atlas (TCGA) and systematically analyzed 19 m6A modulators for their potential significance in RCC. Our aim was to explore the effects and build a prognostic model of m6A modulators in RCC, helping to predict the survival rate of patients and providing further evidence for future research.

## Methods

*Data acquisition*

We downloaded the RNA-seq transcriptome and clinical information data for renal cell carcinoma (RCC) from The Cancer Genome Atlas (TCGA) dataset (https://portal.gdc.cancer.gov/), adhering to the guidelines and policies for acquisition and application. Our studies included 883 cases of RCC. We filtered out all potential m6A-related genes based on Juan Xu's research [1] on the molecular characterization and clinical significance of m6A modulators across 33 cancer types. We also searched GSCALite (http://bioinfo.life.hust.edu.cn/web/GSCALite/) to identify m6A modulators active in cell signaling pathways.

*Survival analysis*

Initially, we extracted information on the 19 m6A RNA methylation modulators and all associated data for further analysis. Utilizing R software packages, namely ggplot2 and pheatmap, we explored the expression distribution, correlation, and heat map of these 19 modulators in both renal cell carcinoma (RCC) and normal tissues. Survival analysis was conducted using the Kaplan-Meier (KM) method, accompanied by a log-rank test to compare the survival differences of the 19 modulators in RCC, as sourced from the TCGA dataset. Overall survival (OS) was assessed using *p*-values and hazard ratios (HR) for the KM curves. A two-sided *P*-value of less than 0.05 was deemed statistically significant. Following the identification of modulators that significantly impacted survival in RCC, we designated these as "Target Genes".

*Consistency clusters analysis*

We utilized the R software package ConsensusClusterPlus (version 1.54.0) to conduct a consistency analysis of "Target Genes". The maximum number of clusters (k) was set to 6, with 80% of the total sample resampled 100 times. The clustering algorithm employed was "hc" (hierarchical clustering) with inner linkage

**Table 1.** Basic characteristics of included patients with renal cell carcinoma

| | Characters | Number |
|---|---|---|
| Status | Alive | 656 |
| | Dead | 227 |
| Age | Mean (SD) | 60.2 (12.4) |
| | Median [MIN, MAX] | 60 [17, 90] |
| Gender | Female | 288 |
| | Male | 595 |
| Race | American Indian | 2 |
| | Asian | 16 |
| | Black | 120 |
| | White | 721 |
| pT_stage | T1 | 79 |
| | T1a | 245 |
| | T1b | 166 |
| | T2 | 95 |
| | T2a | 17 |
| | T2b | 18 |
| | T3 | 13 |
| | T3a | 169 |
| | T3b | 59 |
| | T3c | 3 |
| | T4 | 15 |
| | TX | 4 |
| pN_stage | N0 | 421 |
| | N1 | 43 |
| | N2 | 5 |
| | NX | 414 |
| pM_stage | M0 | 695 |
| | M1 | 91 |
| | MX | 97 |
| pTNM_stage | I | 464 |
| | II | 107 |
| | III | 188 |
| | IV | 103 |
| Grade | G1 | 14 |
| | G2 | 227 |
| | G3 | 206 |
| | G4 | 75 |
| | GX | 5 |

'ward.D2'. The R package pheatmap (version 1.0.12) was utilized to generate clustering heatmaps. The gene expression heatmap retained genes with a standard deviation (SD) greater than 0.1. If the number of input genes exceeded 1,000, the top 25% of genes, sorted by SD, were extracted. Subsequently, survival analysis of different clusters was performed using the Kaplan-Meier method with the log-rank test. Additionally, we used immunedeconv, an R package that integrates six state-of-the-art algorithms (TIMER, xCell, MCP-counter, CIBERSORT, EPIC, and quanTIseq), to perform immune infiltration estimation of different clusters.

*Prognostic significance and predicted model*

The prognostic significance of "Target Genes" was explored using univariate and multivariate Cox regression analyses. The forestplot R package was utilized to visualize the *P*-value, hazard ratio (HR), and 95% confidence interval (CI) for each variable. Based on the outcomes of the multivariate Cox proportional hazards analysis, a nomogram and a risk score model were constructed to predict 1-, 3-, and 5-year overall survival by incorporating these "Target Genes" and clinical factors.

*Enrichment analysis*

Surfing the STRING website (https://string-db.org/), we set the query of "Target Genes", organism ("Homo sapiens"), and main parameters: minimum required interaction score ["Low confidence (0.150)"], the meaning of network edges ("evidence"), max number of interactors to show ("no more than 50 interactors") and active interaction sources ("experiments"). Meanwhile, we uploaded the gene lists to DAVID (Database for annotation, visualization, and integrated discovery), and set them as ("OFFICIAL_GENE_SYMBOL") and species ("Homo sapiens"), and obtained the data of the functional annotation chart. The enriched pathways were finally visualized with the R packages of "tidyr" and "ggplot2". $P<0.05$ was considered statistically significant. Furthermore, we combined the above data to perform in KEGG (Kyoto encyclopedia of genes and genomes) to find the possible pathways.

## Results

*Differential expression and correlation of m6a regulators in RCC*

The clinical characteristics of the included RCC patients are summarized in **Table 1**. Initial analysis of 19 m6A RNA methylation modulators revealed significant differential expression

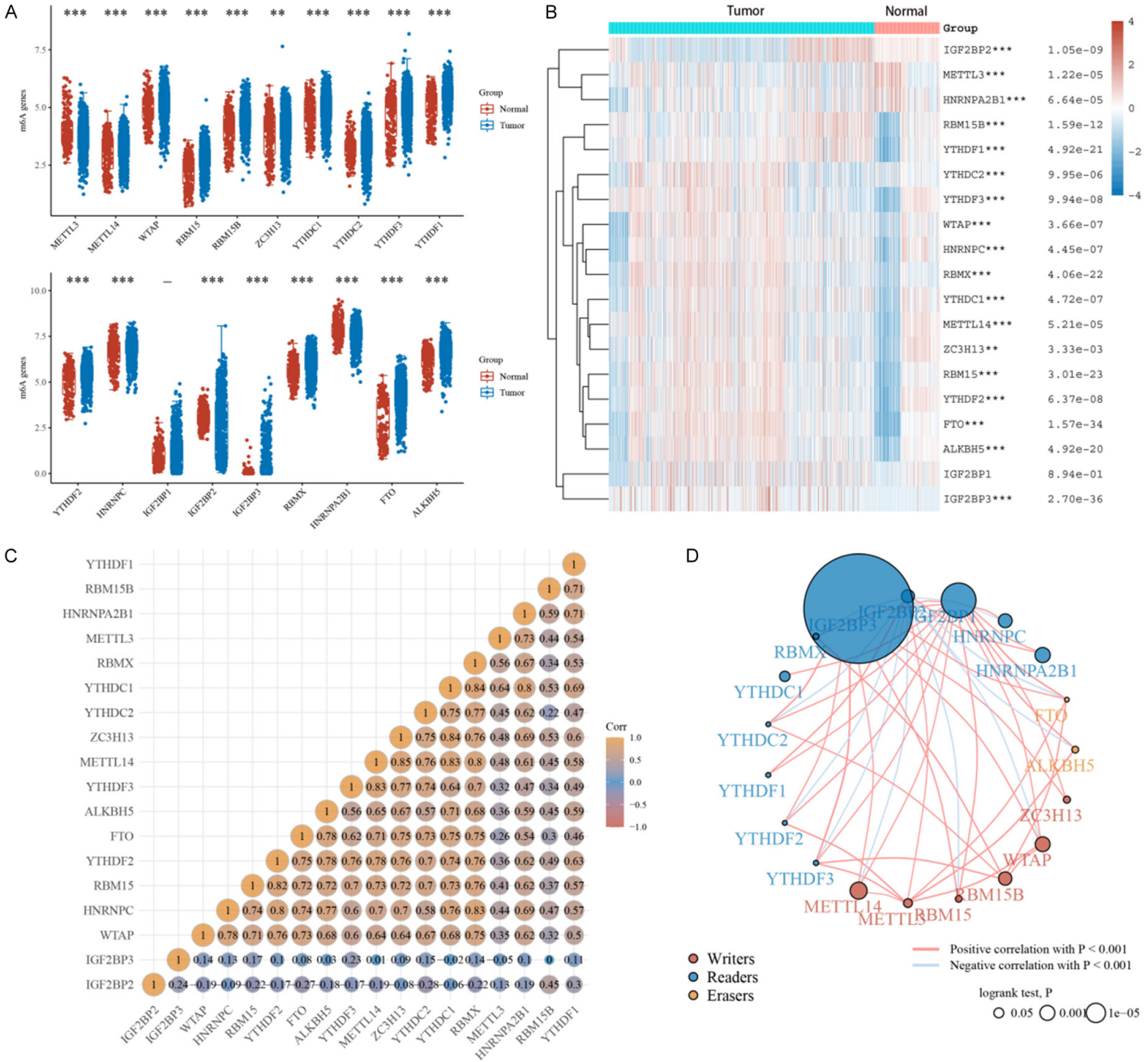
A
B
C
D
Tumor
Normal
Group
m6A genes
METTL3
METTL14
WTAP
RBM15
RBM15B
ZC3H13
YTHDC1
YTHDC2
YTHDF3
YTHDF1
YTHDF2
HNRNPC
IGF2BP1
IGF2BP2
IGF2BP3
RBMX
HNRNPA2B1
FTO
ALKBH5
IGF2BP2*** 1.05e-09
METTL3*** 1.22e-05
HNRNPA2B1*** 6.64e-05
RBM15B*** 1.59e-12
YTHDF1*** 4.92e-21
YTHDC2*** 9.95e-06
YTHDF3*** 9.94e-08
WTAP*** 3.66e-07
HNRNPC*** 4.45e-07
RBMX*** 4.06e-22
YTHDC1*** 4.72e-07
METTL14*** 5.21e-05
ZC3H13** 3.33e-03
RBM15*** 3.01e-23
YTHDF2*** 6.37e-08
FTO*** 1.57e-34
ALKBH5*** 4.92e-20
IGF2BP1 8.94e-01
IGF2BP3*** 2.70e-36
Corr
Writers
Readers
Erasers
Positive correlation with P < 0.001
Negative correlation with P < 0.001
logrank test, P
0.05
0.001
1e−05

**Figure 1.** Expression and correlation of 19 m6A regulators in RCC. A. Expression levels of m6A regulators in RCC and normal tissues based on TCGA and GTEx data. B. m6A regulator expression heatmap in RCC samples. C. Spearman correlation analysis of the 19 m6A regulators. D. Network illustrating the relationships among the 19 m6A regulators.

for 14 regulators between RCC tumor tissues and adjacent normal kidney tissues. Notably, the expression of ALKBH5, KIAA1429, and RBM15B was markedly altered (**Figure 1A**). A subsequent expression heatmap highlighted IGF2BP3 as exhibiting one of the most distinct expression trends, suggesting its potential prominent role in RCC pathogenesis (**Figure 1B**). Correlation analysis among all modulators identified a particularly strong positive correlation between METTL4 and ZC3H13 (**Figure 1C**), a relationship further visualized in a correlation network (**Figure 1D**). The robustness of this METTL4-ZC3H13 co-expression relationship was independently validated using the GEPIA and GEO databases (**Figure 2A**, **2B**), indicating a potentially consistent and biologically relevant interaction between these two regulators in RCC.

*Key m6A regulators are significantly associated with patient survival*

To assess the clinical relevance of the differentially expressed m6A regulators, we performed survival analysis. The expression levels of four modulators - IGF2BP3 (hazard ratio [HR]=2.42, P<0.001), METTL14 (HR=0.758, P=0.038), RBM15B (HR=0.742, P=0.029), and WTAP (HR=1.31, P=0.043) - were significantly associated with overall survival (OS) in RCC patients (**Figure 3**). These results suggest distinct prognostic impacts: high expression of IGF2BP3 and WTAP appears to confer a poorer prognosis (HR>1), whereas high expression of METTL14 and RBM15B may be protective (HR<1). Given their significant association with patient outcomes, these four genes were designated as “Target Genes” for all subsequent investigations.

*RCC patient stratification based on target genes has prognostic value*

Leveraging the expression patterns of the four Target Genes, we performed consensus clustering analysis to stratify RCC patients into biologically distinct subgroups. The analysis determined an optimal division into four consensus clusters (**Figure 4A-D**). Notably, these clusters exhibited significantly different OS rates (P= 0.00013), with Cluster 3 demonstrating the most favorable prognosis and Cluster 1 the poorest (**Figure 5**). This finding confirms that the combined expression profile of these m6A regulators can effectively categorize RCC patients into groups with divergent clinical outcomes, underscoring the prognostic utility of this gene set.

*Construction and validation of a four-gene signature prognostic model*

To quantitatively assess risk, we constructed a prognostic model using LASSO Cox regression based on the four Target Genes (**Figure 6A**, **6B**). The derived risk score formula was: Risk score = (-0.6227) METTL14 + (0.6246) WTAP + (-0.1706) RBM15B + (0.5277) IGF-2BP3. According to the median risk score, patients were stratified into high- and low-risk groups. Survival analysis revealed that patients in the high-risk group had a significantly worse OS probability compared to those in the low-risk group (HR=3.013, P=1.12e-13; **Figure 6C**). This model consolidates the prognostic information of the four individual genes into a single, powerful composite score for outcome prediction.

*Target gene expression is closely linked to the tumor immune microenvironment*

To explore potential mechanisms underlying the prognostic role of the Target Genes, we investigated their relationship with the tumor immune microenvironment. Immune infiltration estimation revealed significant correlations between the expression of several Target Genes and the abundance of specific immune cell types, such as CD4+ T cells, macrophages, and natural killer (NK) cells (**Figure 7**). Furthermore, comparative analysis across the four previously defined consensus clusters showed substantial heterogeneity in the estimated infiltration levels of T cells, B cells, NK cells, and macrophages (**Figure 8**). These results suggest that the prognostic stratifica-

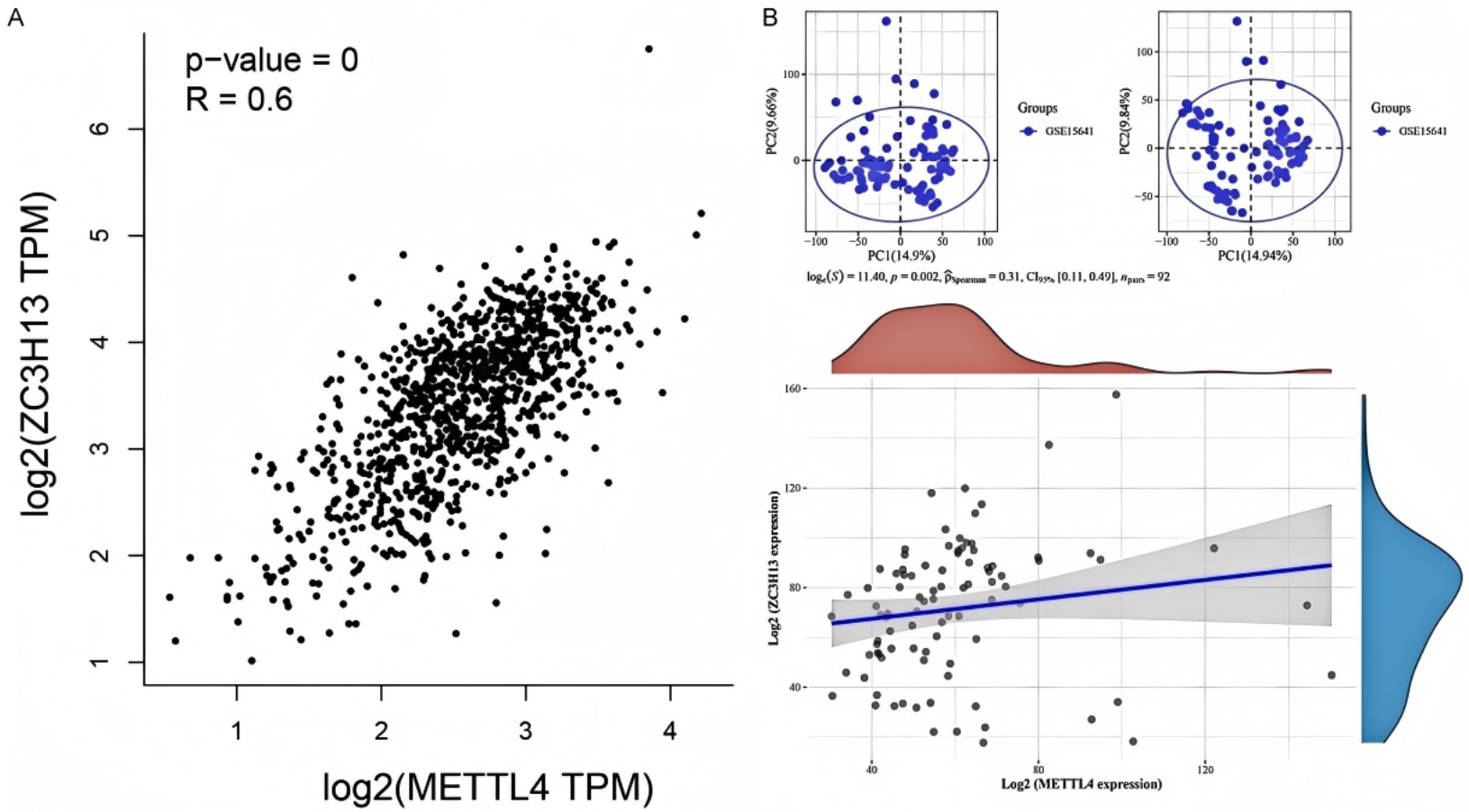


**Figure 2.** Validation of METTL4 and ZC3H13 correlation. A. Relationship between ZC3H13 and METTL4 in RCC based on GEPIA. B. Relationship between ZC3H13 and METTL4 in RCC based on the GEO database.

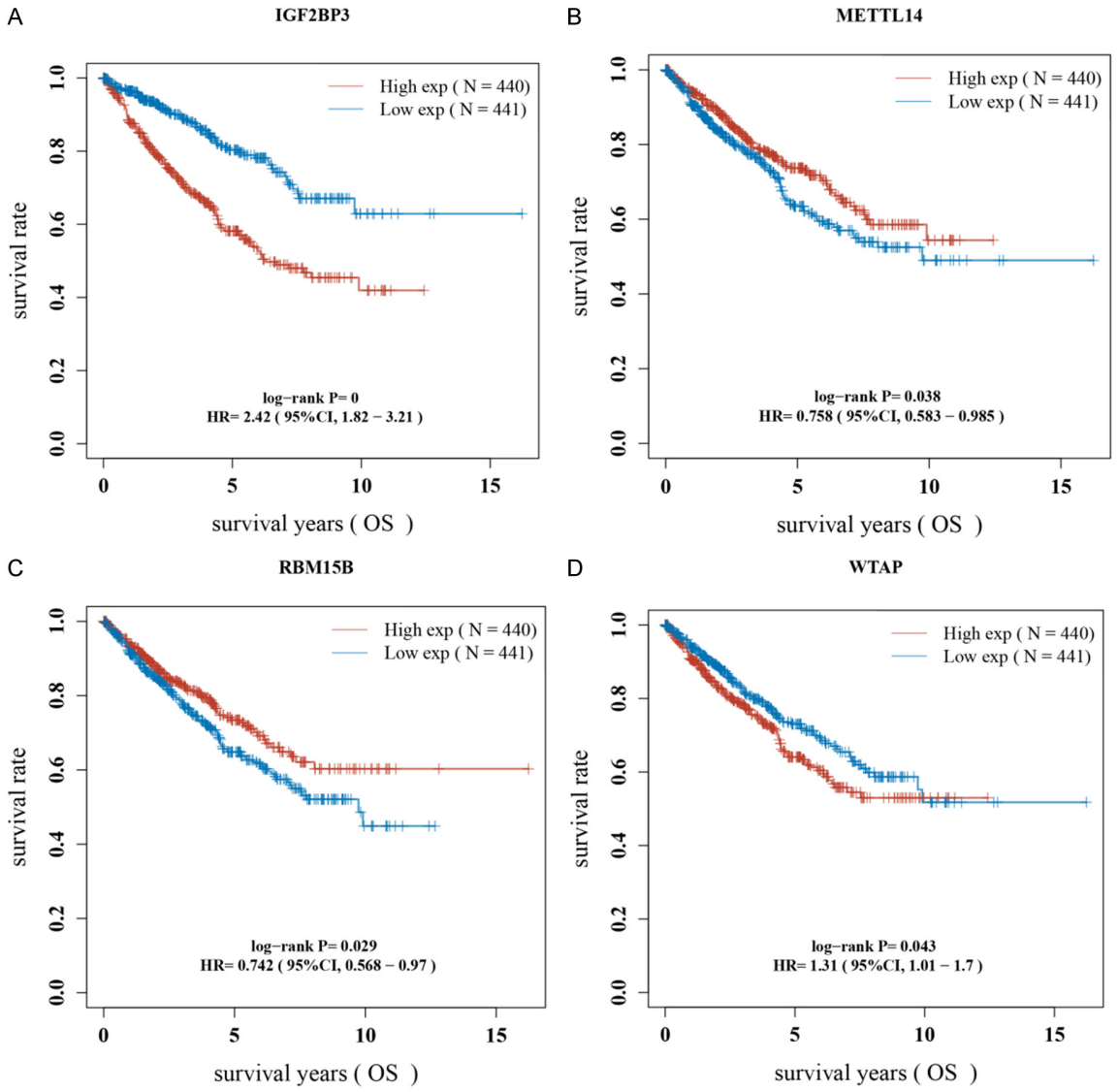


**Figure 3.** Survival analysis of key m6A regulators. Kaplan-Meier survival curves for (A) IGF2BP3, (B) METTL14, (C) RBM15B, and (D) WTAP.

tion driven by m6A regulators may be closely associated with distinct patterns of immune cell infiltration within the tumor.

*Target genes serve as independent prognostic factors and enable nomogram construction*

We next evaluated the independent prognostic value of the Target Genes alongside standard clinicopathological variables. Univariate Cox analysis confirmed METTL14, WTAP, RBM15B, and IGF2BP3 as significant prognostic factors (**Figure 9A**). Importantly, in multivariate analysis, METTL14 (HR=0.665, P=0.024), WTAP (HR=1.397, P=0.044), and IGF2BP3 (HR= 1.354, P<0.001) retained their significance as independent predictors of OS (**Figure 9B**). Integrating these three independent genetic factors with key pathological stages (pM and pTNM), we constructed a practical nomogram to predict 1-, 3-, and 5-year OS probabilities for individual patients (**Figure 9C**). The calibration plots showed excellent agreement between the nomogram's predictions and actual observed outcomes (C-index: 0.701, P<0.001; **Figure 9D**), demonstrating its clinical applicability.

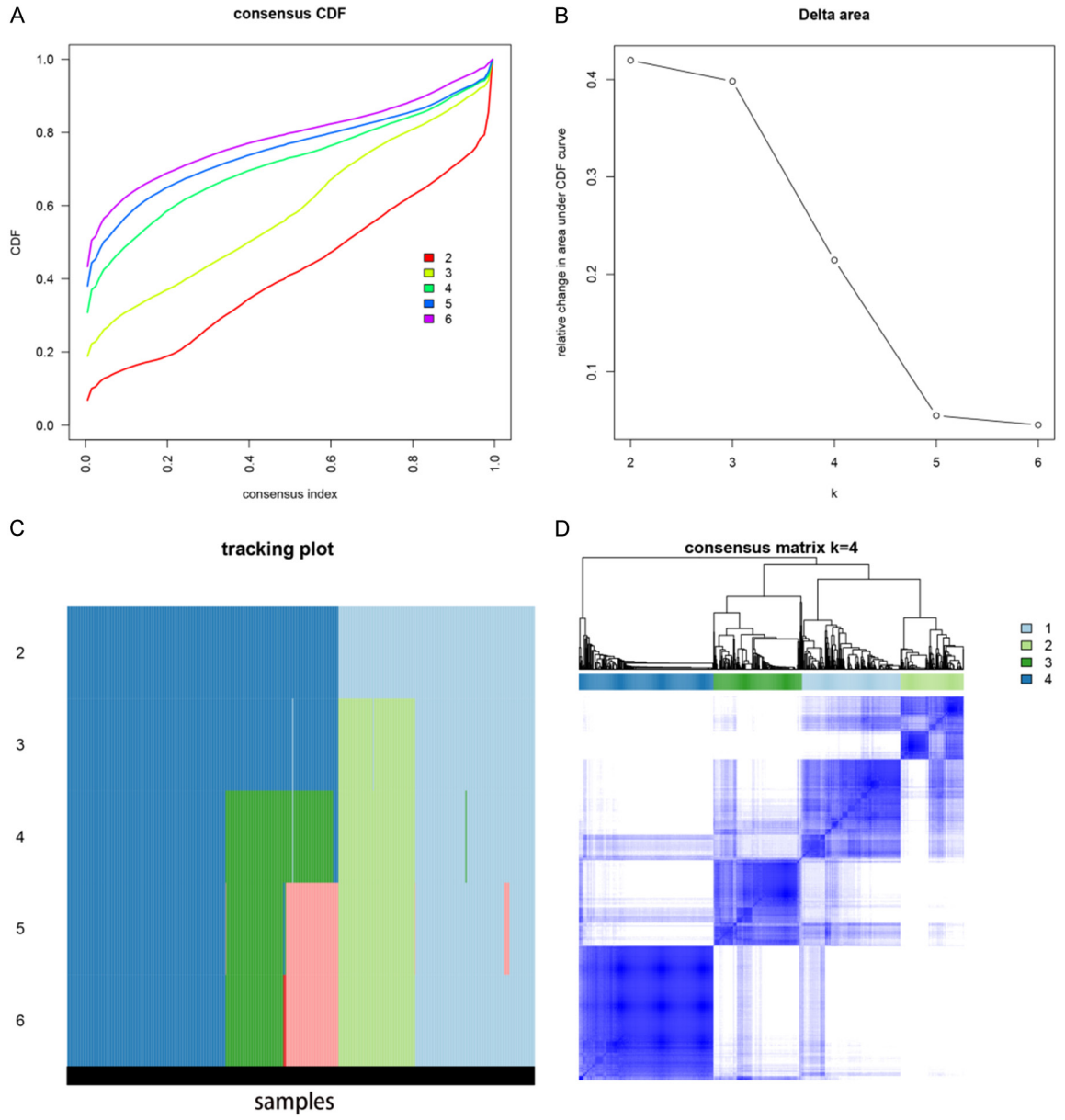


**Figure 4.** Consensus clustering by the four target genes. A. Cumulative distribution function (CDF) for k=2 to 6. B. Delta area under the CDF curve for k=2 to 6. C. Tracking plot of sample clustering. D. Correlation heatmap between the four consensus clusters (k=4).

*Target genes are enriched in key cancer-related pathways*

To elucidate the potential biological functions of the Target Genes in RCC, we performed gene set enrichment analysis. The results indicated that METTL14, WTAP, RBM15B, and IGF2BP3 are implicated in several canonical cancer-associated signaling pathways, including the mTOR, VEGF, Wnt, and p53 signaling pathways (**Figure 10**). This enrichment suggests that these m6A regulators may exert their oncogenic or tumor-suppressive roles by modulating these critical cellular processes involved in growth, angiogenesis, proliferation, and apoptosis.

## Discussion

In this study, we demonstrated that four m6A methylation regulators - METTL14, WTAP, RBM15B, and IGF2BP3 - exert significant

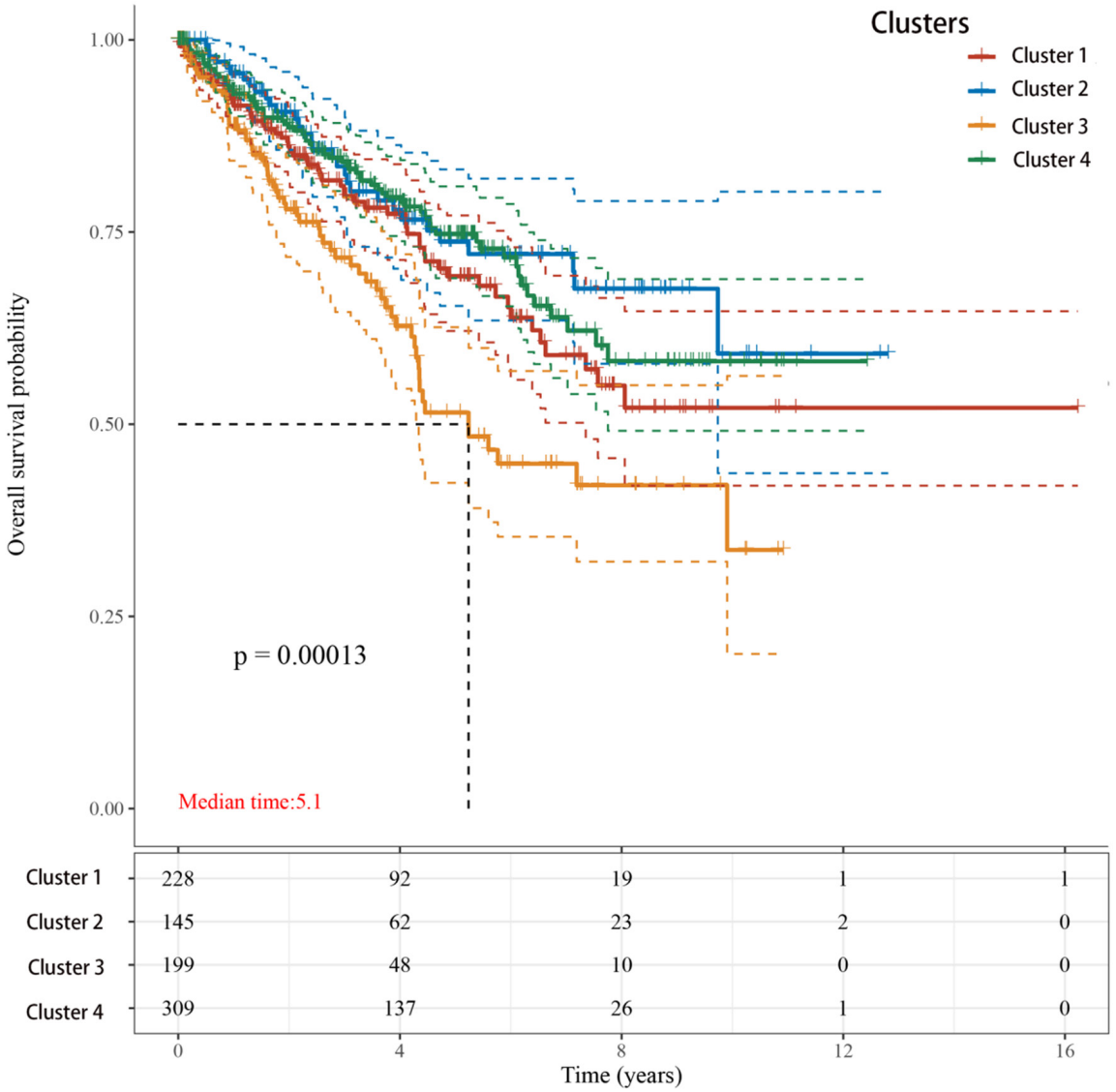


**Figure 5.** Survival analysis of the four consensus clusters. Kaplan-Meier survival curves based on the four clusters identified by the target genes.

effects on the survival of renal cell carcinoma (RCC) and could serve as potential biomarkers for the disease. METTL14, WTAP, and RBM15B, known as "writers", catalyze the formation of m6A; IGF2BP3, via its YTH domain, functions as a "reader" that recognizes and binds m6A, thereby enhancing target mRNA stability. Writers and readers are integral regulators of m6A RNA methylation, playing diverse roles in tumorigenesis and cancer progression.

Our findings align with prior research in other malignancies. For instance, Yang et al. [20] observed that METTL14 knockdown significantly enhanced the proliferative and invasive capacities of colorectal cancer cells while promoting in vivo tumorigenicity and metastasis, with METTL14 loss correlating with poor prognosis. WTAP and RBM15B have been reported to form complexes and mediate m6A methylation in ovarian cancer [21] and gastric cancer [22]. As a reader protein, IGF2BP3 regulates RNA stability, translation, and storage. Recently, Li et al. [23] demonstrated that destabilizing IGF2BPs can activate anti-tumor immunity and inhibit non-small cell lung cancer progression. In our analysis, high IGF2BP3

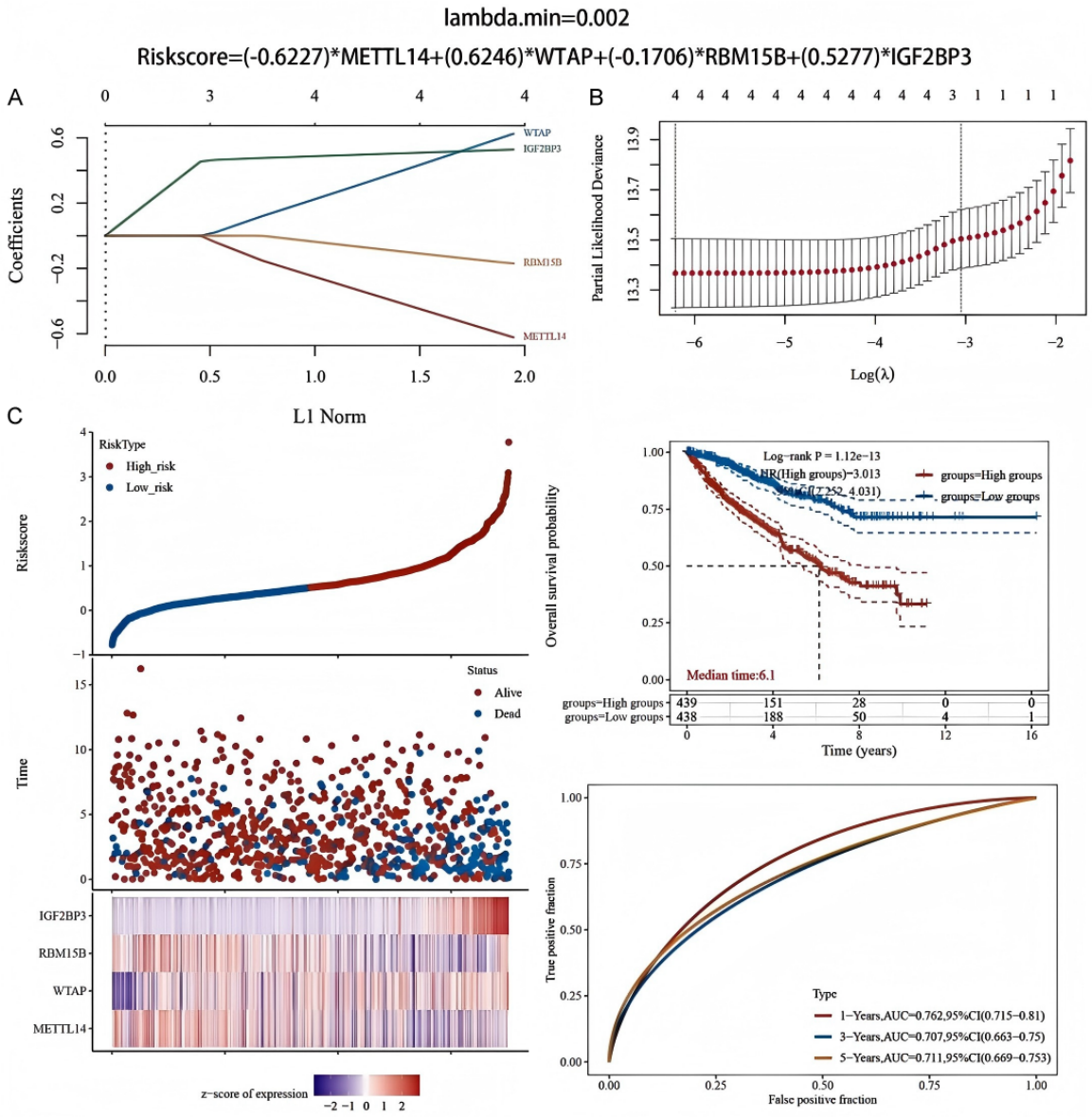


**Figure 6.** Prognostic signature based on the four target genes. A. LASSO coefficient profiles. B. Partial likelihood deviance for the LASSO model. C. Kaplan-Meier survival curves for the high-risk and low-risk groups (left) and time-dependent ROC analysis (right).

expression predicted poor prognosis in RCC, consistent with its established oncogenic role.

Given the intimate link between these m6A regulators and cancer, we performed comprehensive analyses to characterize their functions in RCC. A consensus cluster defined by high-risk profiles of the four regulators exhibited significantly lower overall survival compared to low-risk groups. Immune infiltration analysis suggested their potential involvement in modulating immune activation - a critical component of the tumor microenvironment. Zhang et al. [24] echoed this perspective, noting that evaluating m6A modification patterns can deepen understanding of tumor microenvironment infiltration characteristics and inform more effective immunotherapeutic strategies.

To translate our findings into clinical practice, we developed a predictive model integrating the four regulators with key clinico-

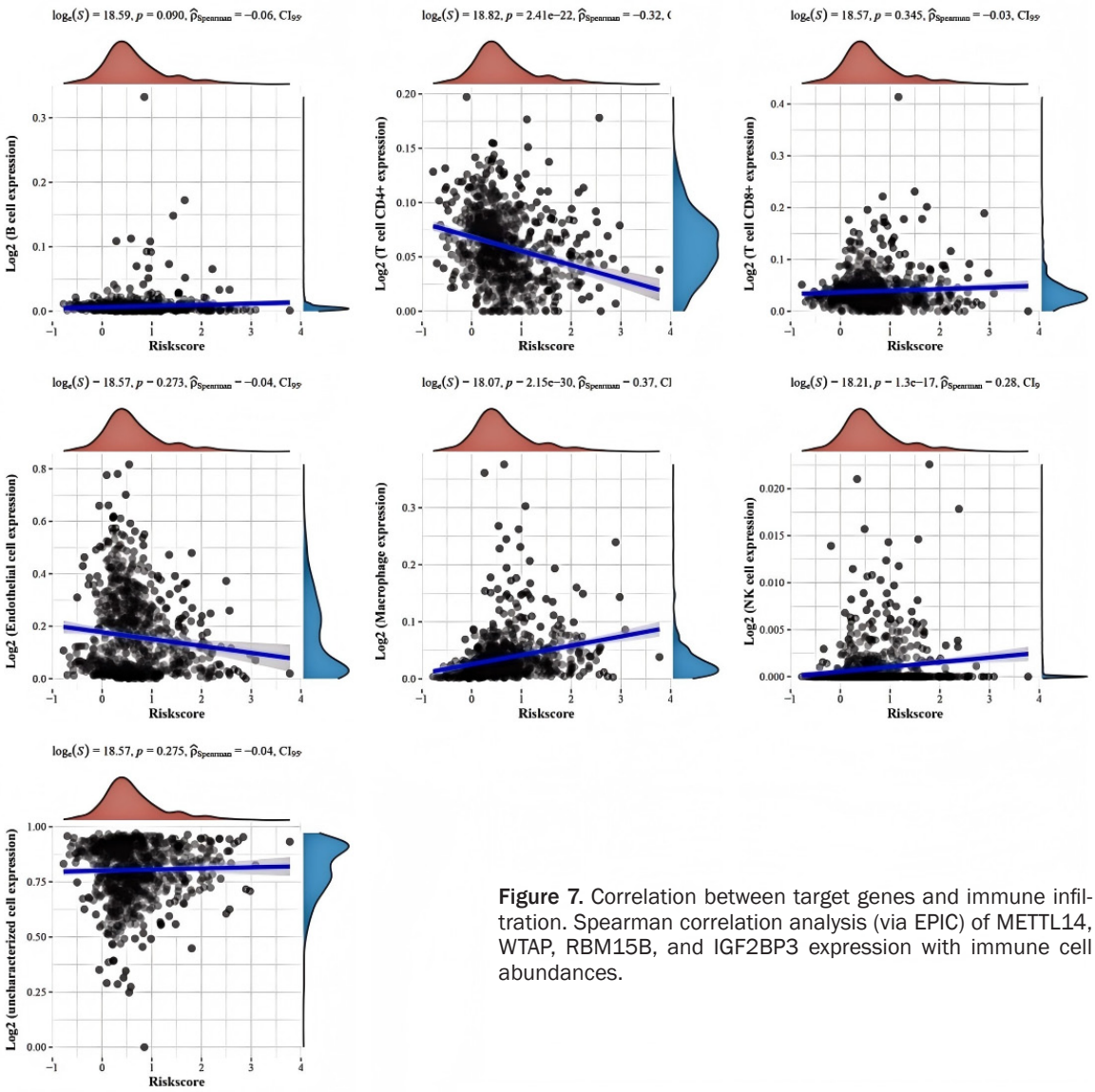


**Figure 7.** Correlation between target genes and immune infiltration. Spearman correlation analysis (via EPIC) of METTL14, WTAP, RBM15B, and IGF2BP3 expression with immune cell abundances.

pathological covariates. Results confirmed the model's robust performance in predicting RCC survival outcomes. We anticipate this work will have clinical utility, providing a valuable reference for comprehensive treatment planning and personalized prognostic assessment.

We acknowledge certain limitations in this study. Despite utilizing multiple databases, additional clinical trials and functional cellular studies are required to validate the precise biological functions of these m6A regulators in RCC. Furthermore, while our findings indicate these regulators participate in the mTOR, Wnt, and p53 signaling pathways, the exact mechanisms by which they modulate RCC tumorigenesis through these pathways warrant further investigation.

## Conclusion

The four m6A methylation modulators - METTL14, WTAP, RBM15B, and IGF2BP3 - have a significant impact on the survival of RCC and could serve as potential prognostic biomarkers. These m6A regulators are involved in key signaling pathways and immune modulation, which play critical roles in the progression of RCC. The established predictive model demonstrates robust performance in stratifying patient risk, highlighting its potential clinical utility.

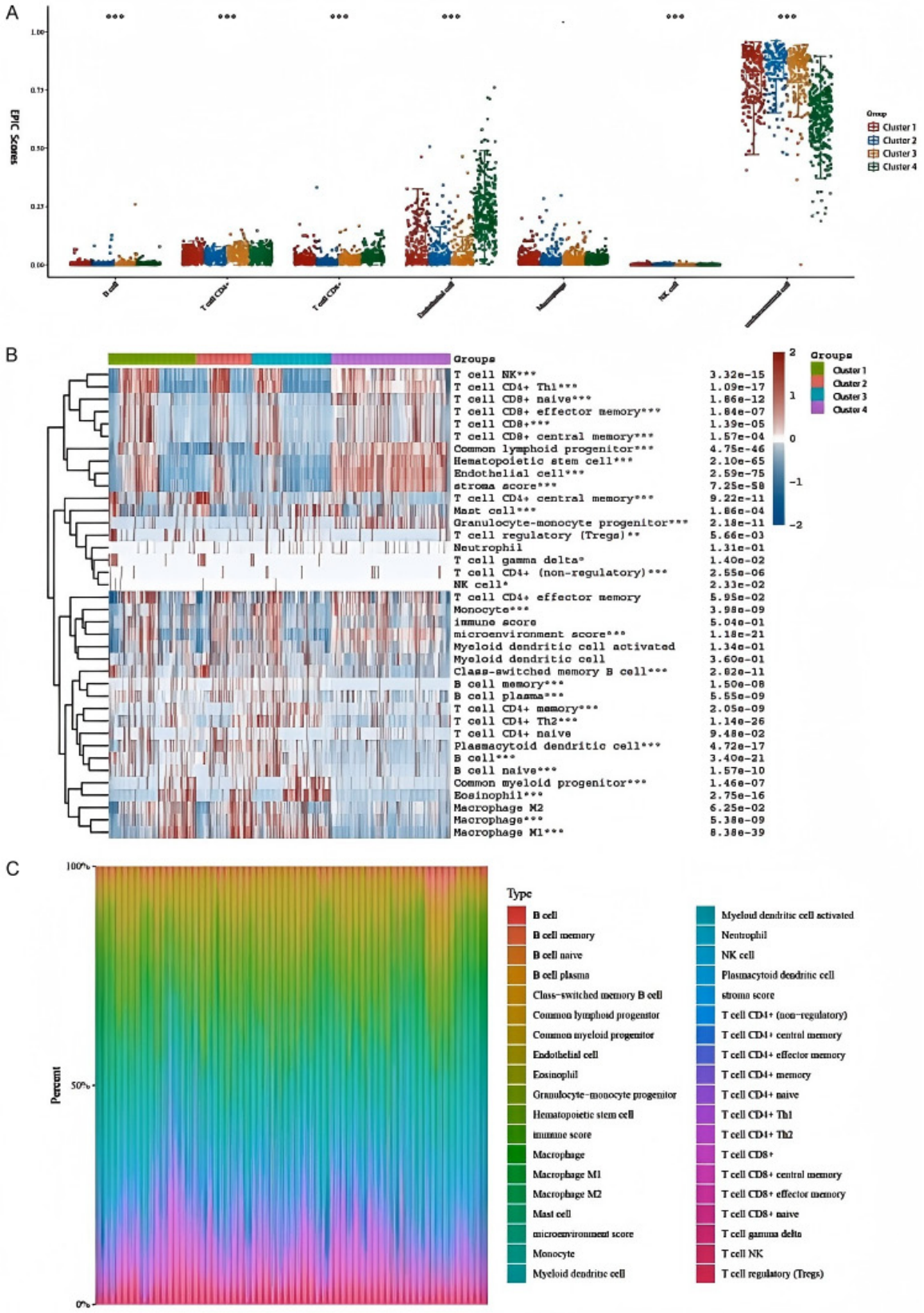


**Figure 8.** Immune infiltration characteristics of the consensus clusters. Immune score distribution of the four clusters in tumor tissues. Heatmap of immune cell scores across the four clusters.

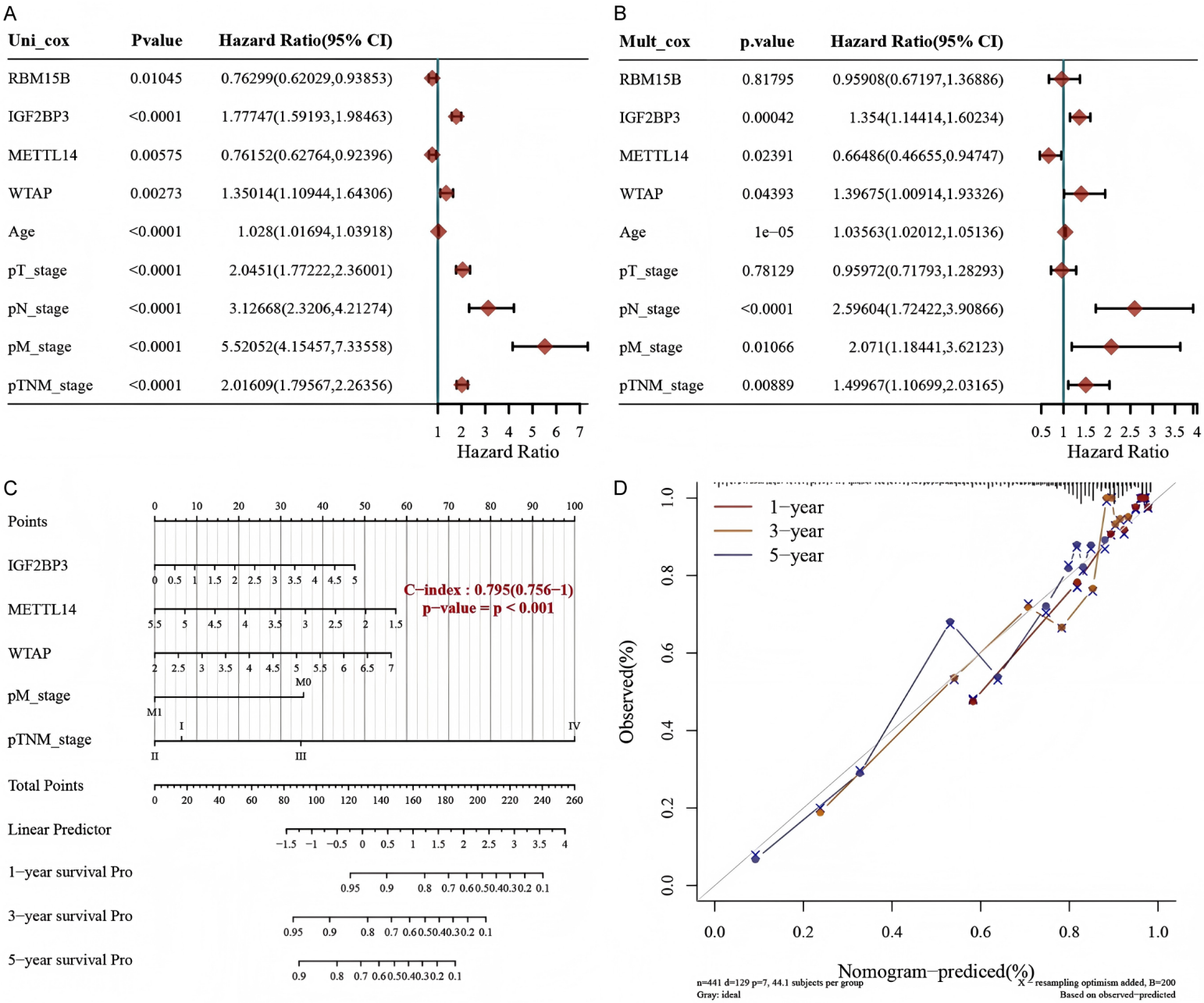
A
Uni_cox Pvalue Hazard Ratio(95% CI)
RBM15B 0.01045 0.76299(0.62029,0.93853)
IGF2BP3 <0.0001 1.77747(1.59193,1.98463)
METTL14 0.00575 0.76152(0.62764,0.92396)
WTAP 0.00273 1.35014(1.10944,1.64306)
Age <0.0001 1.028(1.01694,1.03918)
pT_stage <0.0001 2.0451(1.77222,2.36001)
pN_stage <0.0001 3.12668(2.3206,4.21274)
pM_stage <0.0001 5.52052(4.15457,7.33558)
pTNM_stage <0.0001 2.01609(1.79567,2.26356)
1 2 3 4 5 6 7
Hazard Ratio
B
Mult_cox p.value Hazard Ratio(95% CI)
RBM15B 0.81795 0.95908(0.67197,1.36886)
IGF2BP3 0.00042 1.354(1.14414,1.60234)
METTL14 0.02391 0.66486(0.46655,0.94747)
WTAP 0.04393 1.39675(1.00914,1.93326)
Age 1e−05 1.03563(1.02012,1.05136)
pT_stage 0.78129 0.95972(0.71793,1.28293)
pN_stage <0.0001 2.59604(1.72422,3.90866)
pM_stage 0.01066 2.071(1.18441,3.62123)
pTNM_stage 0.00889 1.49967(1.10699,2.03165)
0.5 1 1.5 2 2.5 3 3.5 4
Hazard Ratio
C
Points
IGF2BP3
METTL14
WTAP
pM_stage
pTNM_stage
Total Points
Linear Predictor
1−year survival Pro
3−year survival Pro
5−year survival Pro
C−index : 0.795(0.756−1)
p−value = p < 0.001
M0
M1
I
II
III
IV
D
1−year
3−year
5−year
Observed(%)
Nomogram−prediced(%)
n=441 d=129 p=7, 44.1 subjects per group
Gray: ideal
resampling optimism added, B=200
Based on observed−predicted

Figure 9. Predictive model and nomogram. (A) Univariate and (B) Multivariate Cox regression analyses of clinicopathological characteristics and the target gene signature. (C) Nomogram predicting 1-, 3-, and 5-year overall survival. (D) Calibration curves for the nomogram.

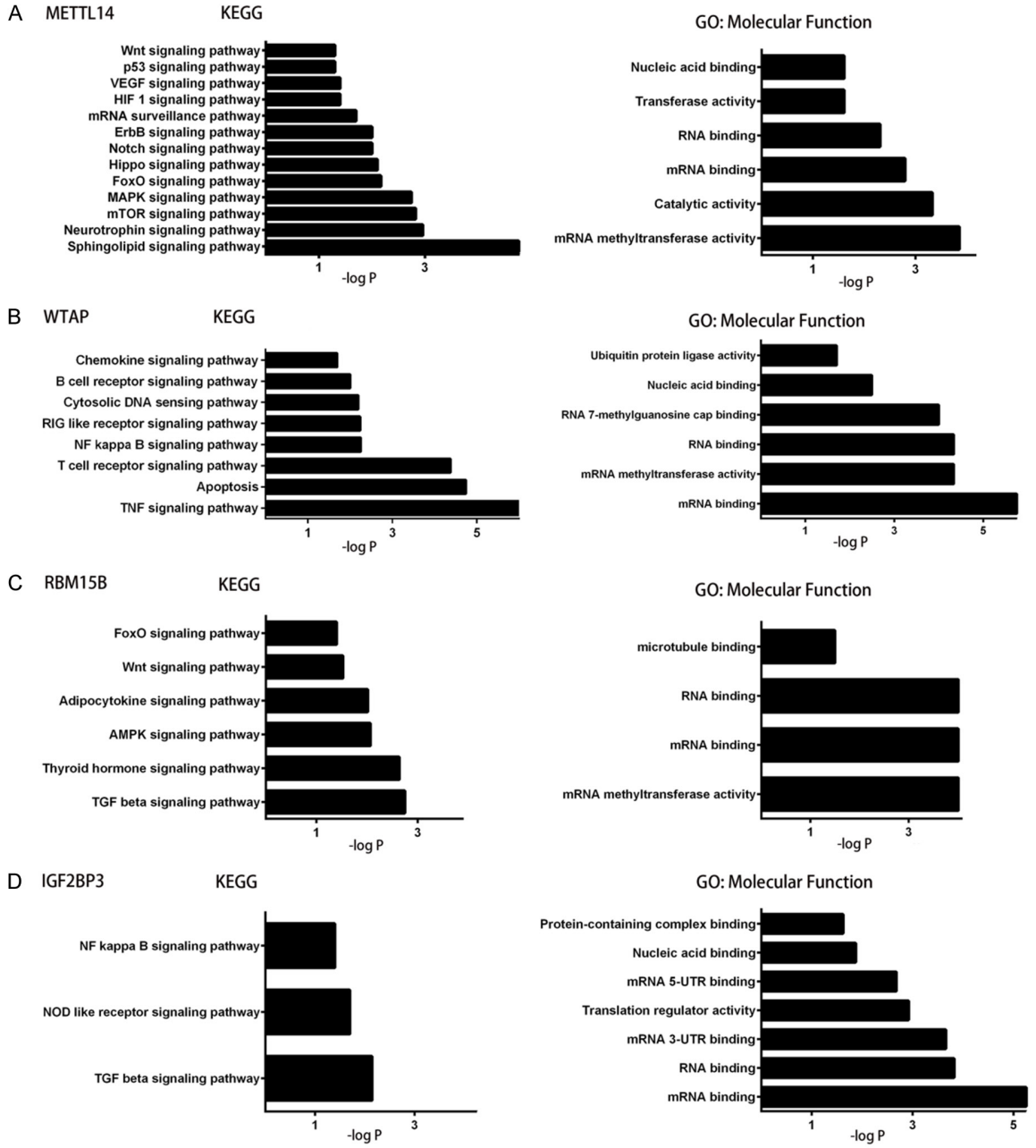


Figure 10. Enrichment analysis of target gene partners. KEGG pathway enrichment analysis for (A) METTL14, (B) WTAP, (C) RBM15B, and (D) IGF2BP3.

## Acknowledgements

This work was supported by Mechanism of CISD1 Regulating GPX4 Ubiquitination-Mediated Ferroptosis in Bladder Urothelial Carcinoma by Yue Yang (Medical Research Project of Chengdu, grant number: 20254-36).

## Disclosure of conflict of interest

None.

## Abbreviations

m6A, N6-Methyladenosine; RCC, Renal cell carcinoma; TIICs, Tumor-infiltrating immune cells; GEPIA, Gene Expression Profiling Interactive Analysis; GTEx, Genotype-Tissue Expression; TPM, Transcripts per million; KM, Kaplan-Meier; HR, Hazard ratio; OS, Overall survival; TMB, Tumor Mutation Burden; MSI, Microsatellite Instability.

**Address correspondence to:** Yue Yang, Urological Department, Affiliated Hospital of Chengdu University, North Road 82#, Chengdu 610081, Sichuan, China. Tel: +86-010-035-88623287; E-mail: sduyangyue@163.com

## References

[1] Siegel RL, Miller KD and Jemal A. Cancer statistics, 2020. CA Cancer J Clin 2020; 70: 7-30.
[2] Padala SA, Barsouk A, Thandra KC, Saginala K, Mohammed A, Vakiti A, Rawla P and Barsouk A. Epidemiology of renal cell carcinoma. World J Oncol 2020; 11: 79-87.
[3] Capitanio U and Montorsi F. Renal cancer. Lancet 2016; 387: 894-906.
[4] Zhu W, Wang JZ, Wei JF and Lu C. Role of m6A methyltransferase component VIRMA in multiple human cancers (Review). Cancer Cell Int 2021; 21: 172.
[5] Chen XY, Zhang J and Zhu JS. The role of m(6) A RNA methylation in human cancer. Mol Cancer 2019; 18: 103.
[6] Haussmann IU, Bodi Z, Sanchez-Moran E, Mongan NP, Archer N, Fray RG and Soller M. m(6)A potentiates Sxl alternative pre-mRNA splicing for robust Drosophila sex determination. Nature 2016; 540: 301-304.
[7] Liu N, Dai Q, Zheng G, He C, Parisien M and Pan T. N(6)-methyladenosine-dependent RNA structural switches regulate RNA-protein interactions. Nature 2015; 518: 560-564.
[8] Huang H, Weng H, Sun W, Qin X, Shi H, Wu H, Zhao BS, Mesquita A, Liu C, Yuan CL, Hu YC, Hüttelmaier S, Skibbe JR, Su R, Deng X, Dong L, Sun M, Li C, Nachtergaele S, Wang Y, Hu C, Ferchen K, Greis KD, Jiang X, Wei M, Qu L, Guan JL, He C, Yang J and Chen J. Recognition of RNA N(6)-methyladenosine by IGF2BP proteins enhances mRNA stability and translation. Nat Cell Biol 2018; 20: 285-295.
[9] Zaccara S, Ries RJ and Jaffrey SR. Reading, writing and erasing mRNA methylation. Nat Rev Mol Cell Biol 2019; 20: 608-624.
[10] Jia G, Fu Y, Zhao X, Dai Q, Zheng G, Yang Y, Yi C, Lindahl T, Pan T, Yang YG and He C. N6-methyladenosine in nuclear RNA is a major substrate of the obesity-associated FTO. Nat Chem Biol 2011; 7: 885-887.
[11] Sun T, Wu R and Ming L. The role of m6A RNA methylation in cancer. Biomed Pharmacother 2019; 112: 108613.
[12] Huang H, Weng H and Chen J. m(6)A modification in coding and non-coding RNAs: roles and therapeutic implications in cancer. Cancer Cell 2020; 37: 270-288.
[13] Li Y, Xiao J, Bai J, Tian Y, Qu Y, Chen X, Wang Q, Li X, Zhang Y and Xu J. Molecular characterization and clinical relevance of m(6)A regulators across 33 cancer types. Mol Cancer 2019; 18: 137.
[14] Li X, Tang J, Huang W, Wang F, Li P, Qin C, Qin Z, Zou Q, Wei J, Hua L, Yang H and Wang Z. The M6A methyltransferase METTL3: acting as a tumor suppressor in renal cell carcinoma. Oncotarget 2017; 8: 96103-96116.
[15] Chi HC, Tsai CY, Tsai MM and Lin KH. Impact of DNA and RNA methylation on radiobiology and cancer progression. Int J Mol Sci 2018; 19: 555.
[16] Capitanio U, Bensalah K, Bex A, Boorjian SA, Bray F, Coleman J, Gore JL, Sun M, Wood C and Russo P. Epidemiology of renal cell carcinoma. Eur Urol 2019; 75: 74-84.
[17] Wang T, Kong S, Tao M and Ju S. The potential role of RNA N6-methyladenosine in cancer progression. Mol Cancer 2020; 19: 88.
[18] Deng X, Su R, Weng H, Huang H, Li Z and Chen J. RNA N(6)-methyladenosine modification in cancers: current status and perspectives. Cell Res 2018; 28: 507-517.
[19] Jiang X, Liu B, Nie Z, Duan L, Xiong Q, Jin Z, Yang C and Chen Y. The role of m6A modification in the biological functions and diseases. Signal Transduct Target Ther 2021; 6: 74.
[20] Yang X, Zhang S, He C, Xue P, Zhang L, He Z, Zang L, Feng B, Sun J and Zheng M. METTL14 suppresses proliferation and metastasis of colorectal cancer by down-regulating oncogenic long non-coding RNA XIST. Mol Cancer 2020; 19: 46.
[21] Yu HL, Ma XD, Tong JF, Li JQ, Guan XJ and Yang JH. WTAP is a prognostic marker of high-grade serous ovarian cancer and regulates the progression of ovarian cancer cells. Onco Targets Ther 2019; 12: 6191-6201.
[22] Li H, Su Q, Li B, Lan L, Wang C, Li W, Wang G, Chen W, He Y and Zhang C. High expression of WTAP leads to poor prognosis of gastric cancer by influencing tumour-associated T lymphocyte infiltration. J Cell Mol Med 2020; 24: 4452-4465.

[23] Li B, Zhu L, Lu C, Wang C, Wang H, Jin H, Ma X, Cheng Z, Yu C, Wang S, Zuo Q, Zhou Y, Wang J, Yang C, Lv Y, Jiang L and Qin W. circNDUFB2 inhibits non-small cell lung cancer progression via destabilizing IGF2BPs and activating anti-tumor immunity. Nat Commun 2021; 12: 295.

[24] Zhang B, Wu Q, Li B, Wang D, Wang L and Zhou YL. m(6)A regulator-mediated methylation modification patterns and tumor microenvironment infiltration characterization in gastric cancer. Mol Cancer 2020; 19: 53.